Contribution of host species and pathogen clade to snake fungal disease hotspots in Europe

Gaëlle Blanvillain[1*], Jeffrey M. Lorch[2], Nicolas Joudrier[3,4,5], Stanislaw Bury[6,7], Thibault Cuenot[8], Michael Franzen[9], Fernando Martínez-Freiría[10,11], Gaëtan Guiller[12], Bálint Halpern[13,14], Aleksandra Kolanek[15,7], Katarzyna Kurek[16], Olivier Lourdais[17,18], Alix Michon[8], Radka Musilová[19], Silke Schweiger[20], Barbara Szulc[7,21], Sylvain Ursenbacher[5,22,23], Oleksandr Zinenko[24] and Joseph R. Hoyt[1]

[1] Biological Sciences Department, Virginia Polytechnic Institute and State University, Blacksburg, VA, USA

[2] U.S. Geological Survey, National Wildlife Health Center, Madison, WI, USA

[3] Institute of Biology, University of Neuchâtel, Neuchâtel, Switzerland

[4] Institute of Animal Pathology, University of Bern, Bern, Switzerland

[5] Info fauna-Karch, Centre Suisse de Cartographie de la Faune (CSCF) and Centre de coordination pour la protection des reptiles et des amphibiens de Suisse (karch), Neuchâtel, Switzerland

[6] Department of Comparative Anatomy, Institute of Zoology and Biomedical Research, Jagiellonian University, Cracow, Poland

[7] NATRIX Herpetological Association, Wroclaw, Poland

[8] LPO Bourgogne-Franche-Comté, Comité territorial de Franche-Comté, Maison de l'environnement de BFC, Besançon, France

[9] Bavarian State Collection of Zoology (ZSM-SNSB), Munich, Germany

[10] CIBIO, Centro de Investigação em Biodiversidade e Recursos Genéticos, InBIO Laboratório Associado, Campus de Vairão, University of Porto, Vairão, Portugal

24 [11] BIOPOLIS Program in Genomics, Biodiversity and Land Planning, CIBIO, Campus de Vairão,
25 Vairão, Portugal
26 [12] Le Grand Momesson, Bouvron, France
27 [13] MME BirdLife Hungary, Budapest, Hungary
28 [14] Department of Systematic Zoology and Ecology, Institute of Biology, Eötvös Loránd University,
29 ELKH-ELTE-MTM Integrative Ecology Research Group, Budapest, Hungary
30 [15] Institute of Geography and Regional Development, Faculty of Earth Sciences and Environmental
31 Management, University of Wroclaw, Poland
32 [16] Department of Wildlife Conservation, Institute of Nature Conservation Polish Academy of
33 Science, Cracow, Poland
34 [17] Centre d'Etudes Biologiques de Chizé, ULR CNRS UMR 7372, Villiers en Bois, France
35 [18] School of Life Sciences, Arizona State University, Tempe, USA
36 [19] Zamenis Civic Association, Karlovy Vary, Czech Republic
37 [20] First Zoological Department, Herpetological Collection, Natural History Museum, Vienna, Austria
38 [21] Department of Genetics, Kazimierz Wielki University, Bydgoszcz, Poland
39 [22] Department of Environmental Sciences, Section of Conservation Biology, University of Basel,
40 Basel, Switzerland
41 [23] Balaton Limnological Research Institute, Tihany, Hungary
42 [24] V.N. Karazin Kharkiv National University, Kharkiv, Ukraine
43
44 *** Corresponding author:** gaelle.blanvillain@gmail.com
45
46 **Keywords:** disease hotspots; fungal pathogen; host-pathogen interactions; *Ophidiomyces*
47 *ophidiicola*; Snake fungal disease

Abstract

1. Infectious diseases are influenced by interactions between host and pathogen, and are rarely homogenous across the landscape. Areas with elevated pathogen prevalence maintain a high force of infection, can facilitate pathogen spread to new regions, and may indicate areas with impacts on host populations. However, isolating the ecological processes that result in increases in infection prevalence and intensity remains a challenge.
2. Here we elucidate the contribution of pathogen clade and host species in disease hotspots of *Ophidiomyces ophidiicola,* the pathogen that causes snake fungal disease, in 21 species of snakes infected with multiple pathogen strains across 10 countries in Europe.
3. We found isolated areas of disease hotspots in a landscape where infections were otherwise low. *O. ophidiicola* clade had important effects on transmission, and areas with multiple pathogen clades had higher host infection prevalence. Snake species identity further influenced infection, with most positive detections coming from the *Natrix* genus. Most species present in the community only experienced increased levels of infection when multiple strains were present. However, one species, *N. tessellata*, appeared highly susceptible, having increased infection prevalence regardless of pathogen strain, indicating that this species may be important in pathogen maintenance.
4. Our results suggest that both host and pathogen identity are essential components contributing to increased pathogen prevalence. More broadly, our findings indicate that coevolutionary relationships between hosts and pathogens may be key mechanisms explaining variation in landscape patterns of disease.

71 **Introduction**

72 Infectious diseases can shape ecological communities by altering host abundance and
73 distributions across the landscape (LaDeau et al. 2007, Holdo et al. 2009, Langwig et al. 2012).
74 Disease outcomes are determined by host-pathogen interactions which are multifaceted and can
75 interact with environmental conditions, creating a mosaic of disease hotspots across broad spatial
76 scales (Krauss et al. 2010, Paull et al. 2012, Brown et al. 2013, Wilber et al. 2020). Hotspots of
77 high pathogen prevalence may represent potential areas of continued impacts to host populations,
78 serve as a source for pathogen dispersal, and maintain high propagule pressure within host
79 communities (Kilpatrick et al. 2006, Krauss et al. 2010, Paull et al. 2012, Brown et al. 2013,
80 Wilber et al. 2020, Laggan et al. 2022).

81 Heterogeneity in innate species susceptibility is recognized as a strong force influencing
82 pathogen transmission and disease impacts for multi-host pathogens (van Riper et al. 1986,
83 LaDeau et al. 2007, Voyles et al. 2009, Langwig et al. 2017). The distribution of highly
84 susceptible species can determine areas of high prevalence if they are critical in pathogen
85 maintenance (Haydon et al. 2002, Ashford 2003). However, the disproportionate contribution of
86 a particular species may be modified by differences in community structure, environmental
87 conditions among patches, and variation in pathogen virulence (Balaz et al. 2014, Wilber et al.
88 2020). Pathogen replication rates can also differ among strains and across the landscape,
89 producing additional variation in disease prevalence (O'Hanlon et al. 2018, Greener et al. 2020).
90 Pathogen strains with high growth rates and virulence may be due to multiple factors, including
91 the introduction of novel strains to new locations or hosts (Li et al. 2004, Becker et al. 2017),
92 ease or independence of transmission from affected hosts (Hawley et al. 2013, Pandey et al.
93 2022), and the development of novel mutations or adaptations that facilitate the escape from host

94 resistance (McLeod and Gandon 2022). Although the interaction between host species and
95 pathogen identity is rarely examined, theory suggests that presence of highly resistant host
96 species could modify the effects of pathogens with high replication rates, creating cold spots of
97 transmission across the landscape (Gandon and Michalakis 2000). Conversely, highly
98 transmissible and virulent pathogen strains in the presence of more moderately affected host
99 species could drive hotspots of infection (Urbina et al. 2018, Ribeiro et al. 2019, McClure et al.
100 2020).

101 The fungal pathogen *Ophidiomyces ophidiicola,* that causes snake fungal disease (SFD,
102 also called ophidiomycosis), has been documented in over 42 species of wild snakes across three
103 continents (Lorch et al. 2016, Burbrink et al. 2017, Franklinos et al. 2017, Meier et al. 2018,
104 Allender et al. 2020, Davy et al. 2021, Grioni et al. 2021, Sun et al. 2021), and is considered a
105 serious threat to the conservation of snake populations (Sutherland et al. 2014, Allender et al.
106 2015). Clinical signs of disease caused by *O. ophidiicola* can range from mild skin lesions, from
107 which snakes can recover, to severe infections that impair movement, disrupt feeding behavior,
108 and can ultimately lead to death (Lorch et al. 2016). Although population declines associated
109 with SFD have been documented in some species of North American snakes (Lorch et al. 2016),
110 no such declines have been reported in species across Europe, where *O. ophidiicola* has most
111 likely coexisted with snakes for longer periods of time (Ladner et al. 2022). However, only
112 limited information is available on *O. ophidiicola* infections across Europe, with just a few
113 individual snakes confirmed to be infected with this pathogen from mainland Europe (Franklinos
114 et al. 2017, Marini et al. 2023, Meier et al. 2018, Origgi et al. 2022).

115 Little is known of the origin of *O. ophidiicola*, and to date, three distinct clades of *O.*
116 *ophidiicola* have been described: clade I, which has been found exclusively in wild snakes in

117 Europe; clade II, which has been reported in wild snakes in North America and Taiwan as well
118 as in captive snakes on multiple continents; and clade III, which has only been found in captive
119 snakes (Ladner et al. 2022). The estimation of the most recent common ancestor between clade I
120 and II (around 2000 years ago), as well as a lack of nonrecombinant intermediates in North
121 America strongly indicate that *O. ophidiicola* was introduced to North America, potentially
122 through multiple introduction events (Ladner et al. 2022). More recently, genotyping from a
123 limited number of samples indicated the presence of both clades I and II in Switzerland dating
124 back to at least 1959 (Origgi et al. 2022). In addition, slower growth rates have been reported for
125 clade I strains of *O. ophidiicola*, suggesting that they may be less virulent than clade II strains
126 (Franklinos et al. 2017). However, prevalence and disease severity associated with the two
127 strains and how they influence landscape patterns of disease has not been directly compared.
128 To investigate the macroecological patterns of SFD across Europe we examined host and
129 pathogen factors that may influence pathogen prevalence and disease severity across the
130 landscape. We evaluated the presence of pathogen hotspots across Europe, examined differences
131 in pathogen prevalence and disease severity among host species, and determined the effect of *O.*
132 *ophidiicola* clade on pathogen prevalence and lesion severity. Finally, we combined host species
133 and pathogen clade to explore factors that may contribute to areas with high pathogen prevalence
134 across the landscape.
135

136 **5. <u>Methods</u>**

137 *(a) Location and host species considered*

138 Free-ranging snakes were captured from March 2020 to June 2022 across 10 countries:
139 Portugal, Spain, France, Switzerland, Germany, Austria, Czech Republic, Hungary, Poland, and

140 Ukraine. The number of sites where snakes were collected ranged from one to nine per country,
141 for a total of 43 sites (Fig. 1, Table S1). Sites were selected based on preexisting geopolitical
142 boundaries within each country (e.g., counties or regions), to account for potential large variation
143 in landscape and geography within each country.
144
145 *(b) Capture and sampling*
146 Snakes were located by visual encounter surveys, an approach frequently used for
147 sampling snakes (Dorcas and Willson 2009). Surveys were guided by pre-existing knowledge of
148 snake presence or prediction of suitable habitats to sample as many species and individuals as
149 possible, and in a wide variety of habitat types. Snakes were captured by hand, placed in
150 individual cloth bags for temporary holding during processing and sampling, and released at their
151 capture location. Sterile handling procedures, including frequent glove changes and
152 decontamination of gear between each snake were followed during sample collection to avoid
153 cross-contamination. Snakes were individually identified using photo-identification or marking
154 (using PIT tags or scale-clipping). For each snake captured, location and morphometric data
155 were collected including latitude/longitude, species, sex, snout-vent-length, tail length, and
156 weight.
157 Snakes were swabbed in duplicate (except for a few individuals that were swabbed only
158 once due to limitations in the field) using a pre-moistened, sterile polyester-tipped applicator
159 (Puritan®, Guilford, Maine, USA) by running the swab five times (back and forth counting as a
160 single pass) on the ventral and dorsal areas (from the neck down to the vent), and two times on
161 the face of the snake. If a skin lesion was observed, a separate swab was used to specifically
162 swab the lesion and skin immediately adjacent to it by rubbing the swab over the affected skin.

163 In addition, for all snakes that had visible lesions, we collected photos for later quantification of
164 infection severity (see below). Swab tips were individually stored in a 2 mL sterile tube in a
165 cooler with ice while in the field, and later stored frozen at -20°C until analysis.
166
167 *(c) Sample extraction and qPCR*
168 A total of 2628 swabs were collected and processed by one of two laboratories following
169 the exact same methods as described below. DNA was extracted from swabs using 250 µL of
170 PrepMan® Ultra Sample Preparation Reagent (Life Technologies, Carlsbad, California, USA)
171 with 100 mg of zirconium/silica beads, following a previously published protocol (Hyatt et al.
172 2007). Briefly, samples were homogenized for 45 sec in a bead beating grinder and lysis system
173 (MP Biomedicals, Irvine, California, USA) and centrifuged for 30 sec at 13000 g to settle all
174 material to the bottom of the tube. Homogenization and centrifugation steps were repeated, and
175 tubes were incubated at 100°C in a heat block for 10 min. Tubes were then cooled at room
176 temperature for 2 min, then centrifuged for 3 min at 13000 g. Fifty to 100 µL of supernatant was
177 recovered and stored at -80°C. Extraction blanks (negative controls) were prepared using 250 µL
178 of PrepMan® Ultra Sample Preparation Reagent and 10 mg of zirconium/silica beads only.
179 Quantitative PCR targeting the internal transcribed spacer region (ITS) specific to *O.*
180 *ophidiicola* was performed on a real-time PCR QuantStudio 5 (Thermofisher Scientific,
181 Waltham, Massachusetts, USA) (Bohuski et al. 2015). QuantiFast Master Mix (QuantiFast Probe
182 PCR + ROX vial kit, Qiagen, Germantown, USA) was prepared according to manufacturer's
183 recommendations for a final reaction volume of 25 µL, which included 5 µL of extracted DNA.
184 Cycling conditions were as follows: 95°C for 3 min, then 95°C for 3 sec and 60°C for 30 sec for
185 a total of 40 cycles. For each plate run, a negative control (water added instead of extracted

186 DNA) and a 6-point (each point run in triplicate) standard curve using synthetic double-stranded
187 DNA (gBlock, Integrated DNA Technologies, Coralville, Iowa) of the target region (1.0×10^2,
188 1.0×10^1, 1.0×10^0, 1.0×10^{-1}, 1.0×10^{-2}, 1.0×10^{-3} fg/µL) were included. Samples that were
189 positive were analyzed in duplicate, and a snake was determined to be positive if any swab
190 associated with that snake was positive by qPCR.
191
192 *(d) Sequencing and genotyping*
193 Samples in which *O. ophidiicola* was detected by qPCR were subjected to follow up
194 genotyping analysis. We targeted a portion of the internal transcribed spacer 2 (ITS2) for this
195 analysis because the ITS2 exhibits variability between previously described clades of *O.*
196 *ophidiicola* and because ITS2 is a multicopy gene that can be amplified from samples containing
197 very small amounts of *O. ophidiicola* DNA (it is also the target of the qPCR assay). We used a
198 nested PCR protocol that consisted of first amplifying the entire ITS2 region with the panfungal
199 primer ITS3 and ITS4 (White et al. 1990). The first reaction consisted of 10 µL of 2x
200 QuantiNova probe PCR master mix (Qiagen, Venlo, Netherlands), 3.9 µL of molecular grade
201 water, 0.5 µL of each primer (20 µM each), 0.1 µL of 20µg/µL bovine serum albumin, and 5 µL
202 of DNA extracted with the PrepMan procedure described above. Cycling conditions were as
203 follows: 95˚C for 3 min; 40 cycles of 95˚C for 10 sec, 56˚C for 30 sec, and 72˚C for 30 sec; final
204 extension at 72˚C for 5 min. For the second reaction, primers ITS3 and Oo-rt-ITS-R (Bohuski et
205 al. 2015) were used. Each reaction consisted of 0.5 µL of the PCR product from the first reaction
206 added to 13.375 µL molecular grade water, 5 µL of GoTaq Flexi buffer (Promega Corporation,
207 Madison, Wisconsin, USA), 2 µL of dNTPs (2.5 mM each), 1.5 µL of 25 mM $MgCl_2$, 1.25 µL of
208 each primer (20 µM each), and 0.25 µL of GoTaq polymerase. Cycling conditions for the second

209 PCR were: 95˚C for 10 min; 45 cycles of 95˚C for 30 sec, 56˚C for 30 sec, and 72˚C for 1 min;
210 final extension at 72˚C for 5 min. Products from the second PCR were visualized on an agarose
211 gel, and those containing bands were sequenced in both directions using the Sanger method with
212 primers ITS3 and Oo-rt-ITS-R.

213 Samples that generated messy chromatograms or appeared to contain single nucleotide
214 polymorphisms (SNPs) indicative of multiple *O. ophidiicola* genotypes were re-amplified with
215 the second PCR using a proofreading polymerase (15.75 µL of molecular grade water, 5 µL of
216 5x SuperFi buffer [Thermo Fisher Scientific Corporation, Waltham, Massachusetts, USA], 2 µL
217 of dNTPs (2.5 mM each), 0.625 µL of 20 µM each primer, 0.5 µL of Platinum SuperFi DNA
218 polymerase [2U/µL], and 0.5 µL of product from the first PCR; cycling conditions were the
219 same as described for the second reaction above). The resulting amplicons were cloned using the
220 Invitrogen Zero Blunt TOPO PCR cloning kit for sequencing (Thermo Fisher Scientific
221 Corporation, Waltham, Massachusetts, USA), and individual transformants were sequenced.

222 Individual ITS2 sequences generated in our study were assigned to genotypes. Sequences
223 with 100% identity across the ITS2 region of *O. ophidiicola* were considered to be the same
224 genotype; any sequence differing from another by at least one SNP was classified as a unique
225 genotype.

226

227 *(e) Quantification of disease severity*

228 Disease severity was measured by calculating the percentage of surface area of each snake
229 covered by lesions. Using the image processing program ImageJ (Schneider et al. 2012) and the
230 photos of the snakes taken in the field, we measured each lesion five times and recorded the
231 mean length and width. We calculated the surface area of each lesion on a particular snake and

232 added up the surface area of each lesion to determine the total lesion surface area. Using the
233 morphometric measurements collected in the field, we also calculated each snake's total surface
234 area from the snout to the tail tip. We then calculated the percentage of total surface area covered
235 by lesions. We also quantified disease severity following a previously described SFD scoring
236 system (Baker et al. 2019) using a combination of lesion type, location, number, and coverage.
237 Scores ranged from 4 (mild) to 12 (most severe). We compared the relationship between lesion
238 score and percentage of total surface area covered by lesions (Fig. S1) and used lesion surface
239 area as a more quantitative measure of severity as opposed to the ordinal metric in the final
240 analyses to describe disease severity.
241
242 *(f) Statistical analyses*
243 We analyzed data using Bayesian hierarchical models and we assessed statistical support
244 using credible intervals that do not overlap zero. We fit all models (unless otherwise noted) using
245 the No-U-Turn Sampler (NUTS), an extension of Hamiltonian Markov chain Monte Carlo
246 (HMCMC). We created all Bayesian models in the Stan computational framework (http://mc-
247 stan.org/) accessed with the "brms" package (Bürkner 2017). To improve convergence and avoid
248 over-fitting, we specified weakly informative priors (a normal distribution with mean of zero and
249 standard deviation of 10), unless otherwise noted. Models were run with a total of 4 chains for
250 2000 iterations each, with a burn-in period of 1000 iterations per chain resulting in 4000
251 posterior samples, which, given the more efficient NUTS sampler, was sufficient to achieve
252 adequate mixing and convergence. All $\hat{R}$ values were less than or equal to 1.01, indicating model
253 convergence. We performed all statistical analyses in R software version 4.2.0 (R Core Team
254 2022).

255 To examine hotspots (i.e., relative disease risk) of the pathogen *O. ophidiicola* across
256 Europe, we used the Getis-Ord Gi* analysis with Local Indicators of Spatial Association (LISA)
257 statistics in the open-source Geographic Information System QGIS (version 3.22.10). A grid map
258 of 100 km x 100 km was created across the landscape to aggregate point data and look at
259 significant spatial clustering of neighboring features (each square) using the resultant z-scores
260 and p-values. A heatmap was created to visualize the *O. ophidiicola* infection risk zone using a
261 kernel density estimation with a quartic kernel shape and kernel radius of 100 km in QGIS. To
262 investigate the effect of host species on pathogen prevalence, we used a Bayesian multilevel
263 model with a Bernoulli distribution, pathogen detection as our response variable (0|1), species as
264 our predictor variables, and a group-level effect of site. We excluded any species that had been
265 sampled fewer than four times. We ran a similar model as described above with genus instead of
266 species and included species as a group-level effect.
267 To investigate differences in lesion prevalence and disease severity in snakes that were
268 qPCR positive, we first ran a multilevel model with a Bernoulli distribution, with detection of
269 lesions on a snake in the field (0|1) as our response variable, species as our predictor variable,
270 and a group-level effect of site. To examine differences in disease severity for the snakes that
271 were positive for *O. ophidiicola,* our response variable was each square millimeter of surface
272 area of the snake, which was treated as Bernoulli trials in a binomial sample (1 = lesion present
273 or 0 = no lesion), and our group-level effects were individual snake and site. We performed a
274 comparison between our lesions severity metric (percent of body covered in lesion) and
275 previously described lesion scoring system (Baker et al. 2019), using a hierarchical model with
276 the scoring system as our response variable, and the fraction of skin covered in lesions as our
277 predictor with a Poisson distribution.

We examined the best model that explained *O. ophidiicola* prevalence across the landscape using leave-one-out cross-validation (LOO). The multilevel models included the population level effects of just species, just pathogen clade, an additive model of species and clade, and an interactive model of species and clade, with a Bernoulli distribution, pathogen detection as our response variable (0|1), and with site as a group-level effect for all four models. Models were run with a total of 4 chains for 6000 iterations each, with a burn-in period of 1500 iterations per chain resulting in 18000 posterior samples. We pooled the four genotypes together (i.e., I-A, I-B, II-D/E and II-F) into two clades (clade I and II) as sample sizes were generally too small across species to look at separately. The clade variable consisted of either clade I (sites where only snakes infected with clade I were detected) or both clades I and II (sites where snakes were infected with either clade I or clade II, as there were only a few locations with detections of only clade II). The final clade dataset used for this analysis included 16 sites and 751 snakes. Prevalence by pathogen clade comparisons are only reported for four species (*N. natrix*, *N. tessellata*, *N. helvetica*, and *Z. longissimus*) for which there was sufficient data. To further examine the contribution of host species and pathogen clade to disease hotspots we also ran the analysis as described above with the addition of a spatial conditional autoregressive (CAR) term in "brms". Finally, to examine how pathogen clade influenced infection severity, we performed an analysis where our response variable was each square millimeter of surface area of the snake, which was treated as a Bernoulli trial in a binomial sample and our predictor was pathogen clade, with a group-level effect of individual snake and species.

6. <u>Results</u>

We captured 1254 individual snakes from 21 species representing 6 genera (Fig. 1, Table S1). A total of 2628 swabs were collected, including 2357 full body skin swabs and 271 lesion swabs. Overall, *O. ophidiicola* prevalence confirmed by qPCR was 8.7% (n = 109 positive snakes) and prevalence was highly variable across the landscape. The hotspot analysis confirmed that sites in Switzerland and across the border in France (Franche-Comte) have elevated pathogen prevalence compared to surrounding areas (99% confidence interval, Z-score ≥ 2.58; $p \leq 0.01$, Fig. 1 and S2), as well as sites sampled in southern Germany, eastern Austria, and eastern Ukraine, but to a lesser extent (95% confidence interval, 1.96 ≤ Z score < 2.58; $0.01 < p \leq 0.05$). Other locations where *O. ophidiicola* was detected (Czech Republic, Hungary, and Poland) were not found to be significant hotspot ($p > 0.05$). Pathogen prevalence was highest in Switzerland (26.7%, Fig. 1, S3), followed by Germany (12.5%, Fig. S3) and Ukraine (12.1%, Fig. S3). Poland and the Iberian Peninsula (Spain and Portugal) had the lowest prevalence at 2.7%, 0.0%, and 0.0% respectively, despite comparable sample sizes to other locations (Table S1).

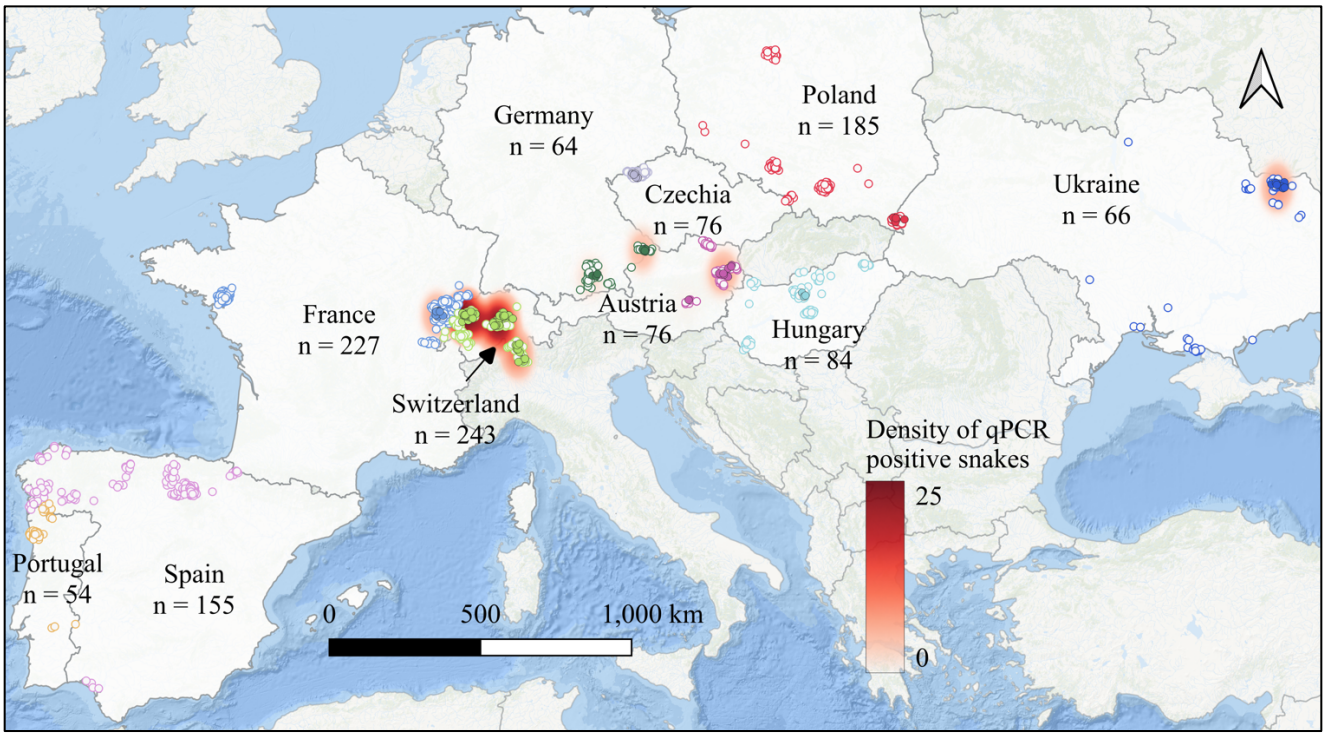

314 **Figure 1. Spatial distribution of snake captures and detections of *O. ophidiicola* across**
315 **Europe.** Each circle represents an individual snake capture and overlapping points were slightly
316 jittered for visualization. Different colors are used to distinguish countries, filled points indicate
317 snakes that were qPCR positive, and outlined points are qPCR negative snakes. Underlying
318 density heatmap shows spatial distribution of *O. ophidiicola* infection risk based on qPCR
319 positive detections using a kernel density estimation algorithm for visualization. We used a 100-
320 km radius around each positive point and the scale bar indicates point density (i.e. relative
321 disease risk) across each region.
322
323 In addition to geographic variation, differences in *O. ophidiicola* prevalence were
324 considerable among hosts (Fig. S4). We found statistical support (results formatted as coefficient
325 ± standard deviation (95% credible intervals)) that species in the *Natrix* genus had higher
326 prevalence (8.2%; intercept: -2.51 ± 0.50 (-3.62, -1.67)) than other genera sampled (0.7%,
327 *Coronella* coeff: -3.13 ± 1.23 (-6.07, -1.24); 0.3%, *Dolichophis* coeff: -8.64 ± 5.60 (-22.53, -
328 0.99); 0.2%, *Vipera* coeff: -4.05 ± 0.87 (-5.95, -2.53)), except for *Hierophis* and *Zamenis* (4.2%
329 and 5.9 %, coeffs: -0.81 ± 0.48 (-1.79, 0.10) and -0.41 ± 0.43 (-1.27, 0.39), respectively). There
330 was also large variation in pathogen prevalence among congeneric species. *Natrix tessellata* had
331 higher *O. ophidiicola* prevalence (model prediction: 15.8 ± 6.2%; Fig. 2 and Table S2) compared
332 to several other members of the *Natrix* genus including *Natrix astreptophora* (0.6%, coeff: -8.5 ±
333 5.8 (-21.77, -0.39)), and *Natrix maura* (2.0%, coeff: -2.66 ± 1.31 (-5.7, -0.56), but there was no
334 statistical support for differences from *Natrix helvetica* (13.7%, coeff: -0.16 ± 0.38 (-0.9, 0.58))
335 or *Natrix natrix* (7.6%, coeff: -0.75 ± 0.49 (-1.73, 0.23)); Fig. 2 and Table S2).

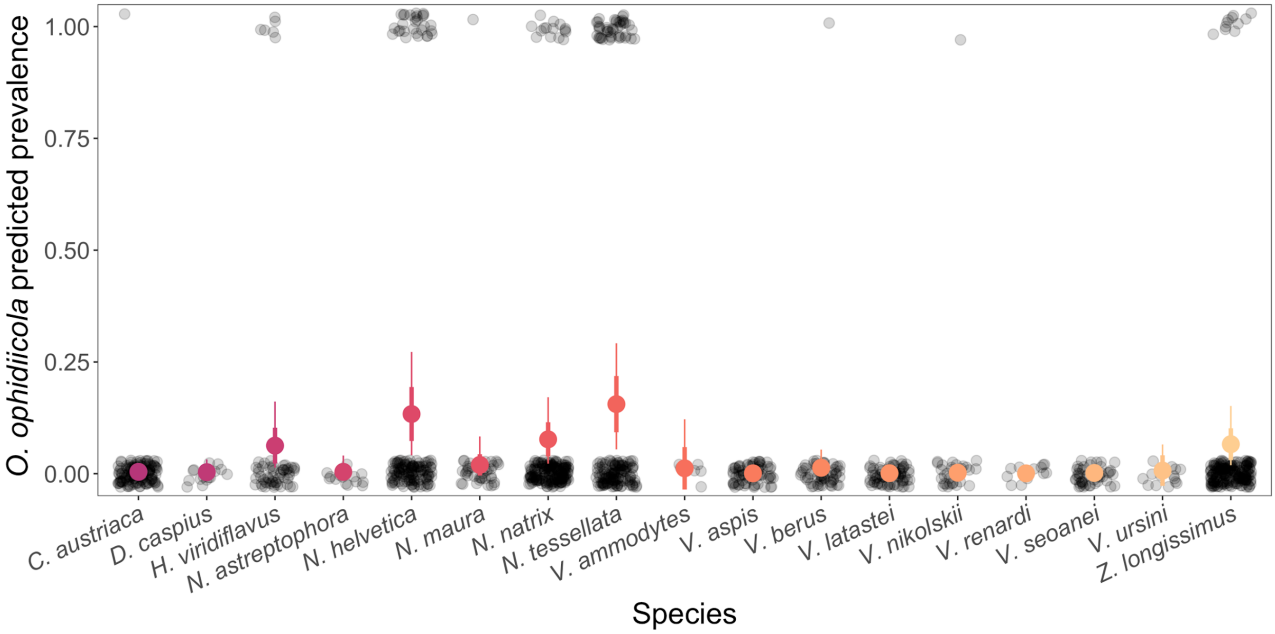

Figure 2. Prevalence of *O. ophidiicola* in different species of snakes across Europe. Each black circle represents a single snake as being either negative (0) or positive (1), which was then used to calculate pathogen prevalence (fraction of the population that was positive). Larger circles and whiskers show the model predicted posterior mean ± standard deviation (thick lines), and 95% credible intervals (thin lines) for each species across all countries. Colors indicate different species.

Overall, skin lesions were observed in 187 snakes from 15 species across all countries, but only 46.5% of those tested positive by qPCR (n = 87). Of all the snakes that tested positive by qPCR (n = 109), 80% of those had skin lesions that were consistent with SFD, while the other 20% had no visible skin lesion (n = 22) (Fig. 3a, Fig. S5). We found a high probability of finding lesions on a snake if they tested positive for *O. ophidiicola* (range 46.2% – 92.8%, except for two viper species which had no visual sign of disease, Fig. 3a). We observed variation in disease severity but no statistical support for differences among species (Fig. 3b, Table S3).

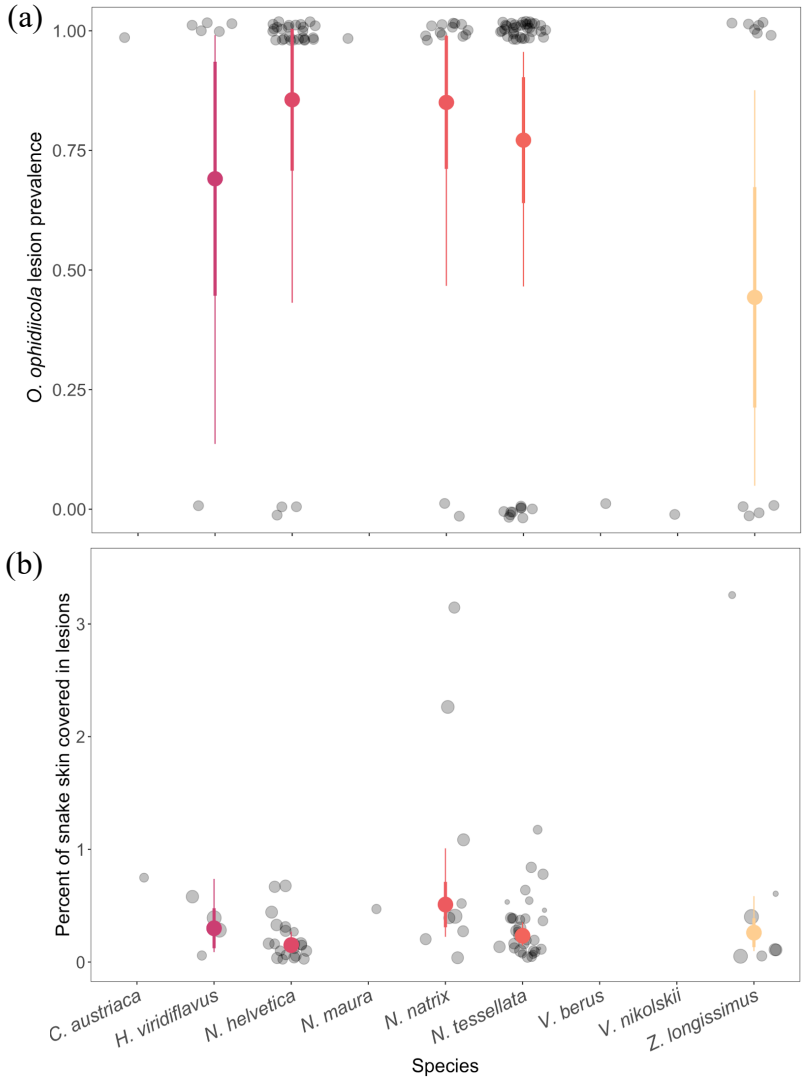

Figure 3. Lesion prevalence (a) and disease severity (b) in *O. ophidiicola*-positive snakes across different species. Color circles and whiskers show the model predicted posterior mean, ± standard deviation (thick lines), and 95% credible intervals (thin lines) for different species across all countries. (a) Each black circle represents a single snake as being either negative (0) or positive (1) for presence of lesions, which was used to calculate the proportion of the population that tested positive (prevalence). (b) Each black circle represents the percentage of the body of a

373 single snake covered in lesions and the size of the circle is proportional to the total surface area
374 of the snake (scale ranges 250 – 1,000 cm^2).
375
376 Genotyping analyses were successful for 85.3% of positives swabs (93 total swab
377 samples) that were qPCR positive for *O. ophidiicola*. A total of four unique genotypes were
378 observed, belonging to two of the major *O. ophidiicola* clades (clade I & II, (Ladner et al. 2022))
379 (Table S4). Two of these genotypes (designated here as I-A and I-B) resided within clade I (i.e.,
380 the "European clade"). What we refer to as genotype I-A had an ITS2 sequence identical to
381 strains previously isolated from Great Britain, while genotype I-B had an ITS2 region sequence
382 identical to a strain from Czechia (Franklinos et al. 2017). The remaining two genotypes that we
383 observed in our study resided within clade II (i.e., the "North American clade") and were
384 identical to ITS2 region sequences of clonal lineages II-D/E (lineages D and E have identical
385 sequences in the ITS2 region) and II-F (Ladner et al. 2022). Here we refer to these genotypes as
386 II-D/E and II-F, respectively, although strains detected in this study may not be true
387 representatives of the clonal lineages reported from North America since recombinant strains can
388 have identical ITS2 sequences as clonal lineages (Ladner et al. 2022). We found that both clade I
389 and clade II are present across much of continental Europe, ranging from eastern France to
390 eastern Ukraine; however, both clades were not present in all locations where *O. ophidiicola* was
391 detected. Genotype I-A was detected primarily in western Europe (Switzerland, Germany, and
392 Austria), whereas genotype I-B was detected in eastern Europe (Czechia, Austria, Hungary,
393 Poland, and Ukraine) (Fig. 4a). Genotype II-D/E was more widely distributed across Europe,
394 whereas genotype II-F was only found along a single lake in Switzerland (Fig. 4a). On two
395 occasions, snakes were found to be infected with multiple genotypes of *O. ophidiicola*: a snake

from Switzerland from which genotypes I-A and II-D/E were detected and a snake from Hungary from which genotypes I-A and I-B were detected.

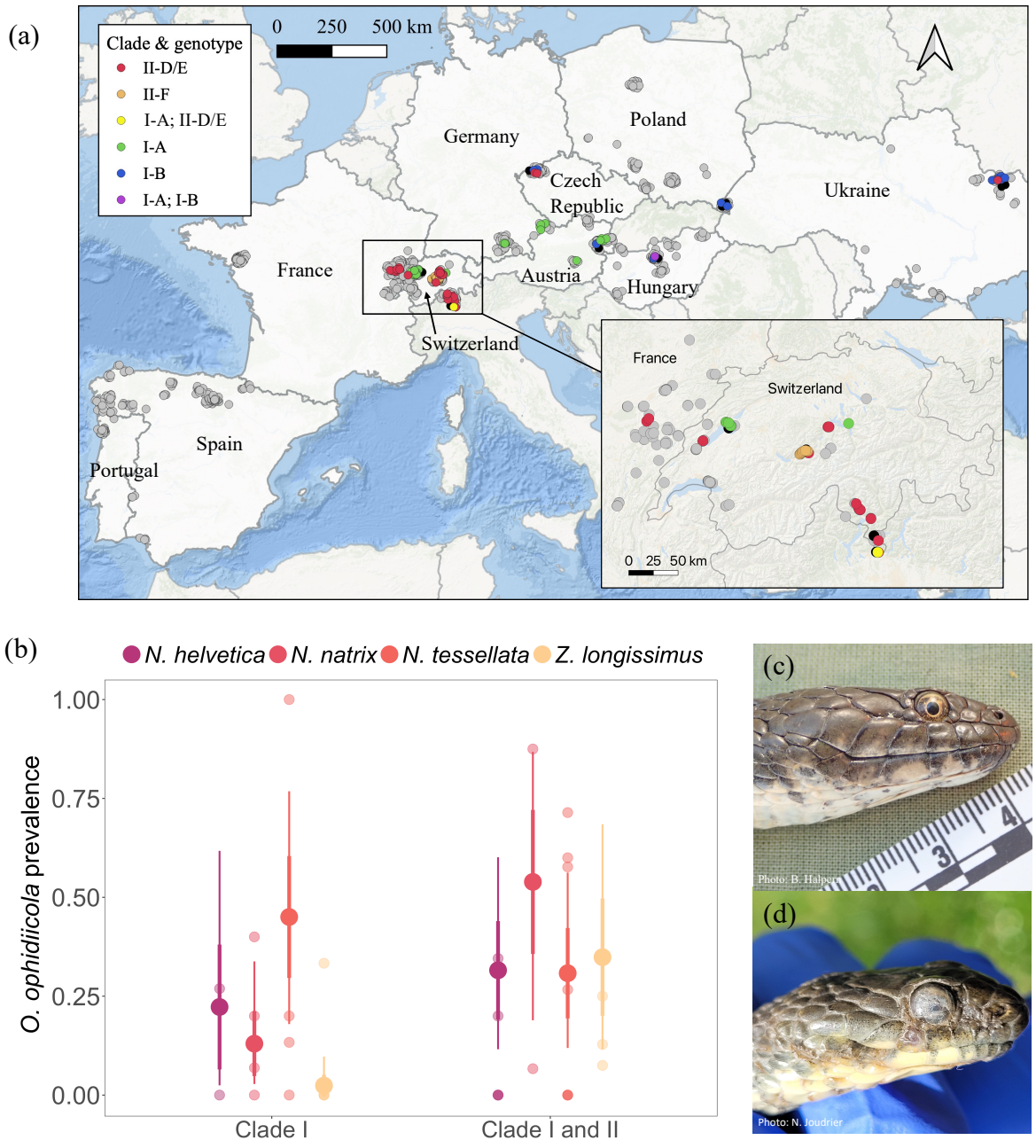

Figure 4. Distribution of *O. ophidiicola* clades across Europe. (a) *O. ophidiicola* clades and lineages from positive detections across the landscape in Europe. Points are slightly jittered for better visual representation of the sampling range. Color of the point indicates the clades and

genotypes, samples that were qPCR negative are represented as grey points, and samples that failed to amplify with the genotyping PCR are represented as black points. Yellow and purple points represent simultaneous detections of genotypes I-A and II-D/E and genotypes I-A and I-B, respectively, from the same swab sample (i.e., snakes infected with multiple genotypes). The enlarged map (inset) shows better resolution of detections in Switzerland. (b) *O. ophidiicola* prevalence across snake species based on *O. ophidiicola* clade presence at the different sites. Small color points are mean prevalence at a site for a given species and clade. Large color points and whiskers show the model predicted posterior mean, ± standard deviation (thick lines), and 95% credible intervals (thin lines) across different species. (c) Photo of a *N. tessellata* from Hungary infected with *O. ophidiicola* from clade I-B. (d) Photo of a *N. tessellata* from Switzerland infected with *O. ophidiicola* from clade II-F showing facial infection.

The top two models, as determined through LOO, that best predicted *O. ophidiicola* prevalence across the landscape included both host species and pathogen clade as predictor variables, with the best fit model including an interaction between these two variables (Table S5). There was statistical support that *N. natrix* and *Z. longissimus* have higher probabilities of being infected when clade II was detected at a site compared to just clade I (*N. natrix* coeff: 2.09 ± 1.09 (0.05, 4.27), *Z. longissimus* coeff: 3.15 ± 1.23 (0.84, 5.69)). A third species, *N. helvetica*, was associated with higher probability of infection when clade II was detected at a site, but the credible intervals included zero (coeff: 0.64 ± 1.16 (-1.59, 3.03)). Conversely, we found that the species with the highest pathogen prevalence, *N. tessellata,* had no differences in infection probability based on clade (Fig. 4b, Table S6). Results from the spatial regression resulted in qualitatively similar results, where both species present and pathogen clade were important

442 predictors of pathogen prevalence (*N. natrix* coeff: 1.10 ± 0.75 (-0.73, 2.35), *Z. longissimus*
443 coeff: 1.74 ± 0.85 (0.10, 3.44), *N. helvetica* coeff: 0.09 ± 0.44 (-0.72, 0.95)), except for *N.*
444 *tessellata* (coeff: -0.59 ± 0.54 (-1.66, 0.42)) (Table S7). Snakes that were infected by a strain of
445 *O. ophidiicola* belonging to clade I generally had less severe disease when compared to snakes
446 infected with a strain from clade II, although there was no strong statistical support as the
447 credible intervals overlapped zero (clade I coeff: -0.10 ± 0.34 (-0.77, 0.57), Fig. S6).
448

449 **4. <u>Discussion</u>**

450 Our results support the presence of hotspots for SFD across Europe and the potential
451 factors that contribute to higher infection prevalence. *O. ophidiicola* was detected in all countries
452 studied except for those on the Iberian Peninsula (Spain and Portugal), which may be attributed
453 to numerous factors (e.g. different species community, geographical barriers (Pyrenees
454 mountains), or environmental conditions) that may be unsuitable for persistence and growth of
455 *O. ophidiicola*. Our surveys establish four regions with elevated prevalence of *O. ophidiicola* in
456 Europe, with the highest being in Switzerland.

457 Snake fungal disease has garnered much attention over the last few decades, as this
458 disease has negatively affected snake populations (Allender et al. 2015, Lorch et al. 2016).
459 Despite this, few studies have systematically examined differences in disease severity and
460 prevalence across species. We found high variability of infection prevalence among snake
461 species, irrespective of the sampling location. Snakes in the *Natrix* genus had a higher
462 probability of infection compared to other genera, indicating that species in this genus may be
463 more susceptible to *O. ophidiicola* infections and are likely to be important in maintaining
464 elevated pathogen prevalence in a region. Underlying host characteristics such as dependence on

465 aquatic habitats, have previously been found to be associated with higher *O. ophidiicola*
466 infection prevalence (McKenzie et al. 2019), which could partly explain increased infection in
467 this genus. *Natrix tessellata* had the highest pathogen prevalence, followed by *N. helvetica* and
468 *N. natrix*, with all three species being either semiaquatic or living near water (with *N. tessellata*
469 being more piscivorous). Interestingly, only two vipers (out of a total of 341 samples) tested
470 positive for *O. ophidiicola*, and both snakes had no visual signs of infection (i.e. no lesions
471 present). This indicates that viperids may not be competent hosts for *O. ophidiicola*, possibly due
472 to environmental associations or behavioral and physiological mechanisms. Contrary to this,
473 North American pit vipers, such as the massassauga rattlesnake (*Sistrurus catenatus*), have been
474 reported to develop severe clinical signs of SFD (Allender et al. 2011). This could be attributed
475 to a sampling bias from more intensive monitoring of threatened rattlesnake species, or
476 rattlesnakes may have increased susceptibility to SFD due to their habitat requirements
477 (massassauga rattlesnakes are found near swamps and marshes) compared to European vipers,
478 which are generally associated with drier environments (except for *V. berus* which can be
479 associated with cool and humid habitats).

480 In our study, no mortality was reported, and snakes generally appeared healthy except in
481 a few cases where infection was severe and had spread to the face with possible disruption to
482 foraging behavior (Fig. S4). The low disease severity observed in Europe could be the result of
483 increased host resistance or generally lower pathogen virulence. We also found that only 46% of
484 snakes with lesions tested positive for *O. ophidiicola*, which has also been reported from North
485 America (Chandler et al. 2019, Haynes et al. 2020). The lesions that could not be attributed to *O.*
486 *ophidiicola* infection looked similar to SFD skin lesions and may be fungal or bacterial in origin

487 (Dubey et al. 2022). Further research investigating other sublethal effects of SFD and the
488 interaction between *O. ophidiicola* and other pathogens is important.

489 We found that models accounting for both host species and pathogen clade best explained
490 the variation in pathogen prevalence across the landscape. Importantly, the top model included
491 an interaction between host species and pathogen clade, indicating that the effect of clade is not
492 the same across species. Clade II was found in two of the four pathogen hotspots across Europe,
493 and generally when clade II was present in an area, we found support that the probability of
494 detecting *O. ophidiicola* was higher for three (*N. natrix*, *Z. longissimus*, and *N. helvetica)* of the
495 four species with the highest prevalence. Hotspots in Switzerland were primarily driven by *N.*
496 *tessellata*, which showed no difference in detection based on whether just clade I or both clades I
497 and II were present. This indicates that *N. tessellata* may be equivalently susceptible to both
498 clades I and II or that other factors may be contributing to infection probability in this species.

499 The history and origin of *O. ophidiicola* in Europe is unclear. Sampling of museum
500 specimens has revealed that strains of *O. ophidiicola* belonging to clades I and II were present in
501 Switzerland as early as 1959 (Origgi et al. 2022). It is estimated that clade I shared a common
502 ancestor within the last 100 to 500 years, but that analysis only included four clade I strains and
503 may greatly underestimate the time that *O. ophidiicola* has been present in Europe (Ladner et al.
504 2022). Despite the designation of clade II as the "North American" clade, it is believed that *O.*
505 *ophidiicola* is not native to North America and multiple introductions (most likely from Eurasia)
506 have occurred over the last century (Ladner et al. 2022). Thus, it is plausible that either or both
507 clades I and II are native to Europe. Strains of *O. ophidiicola* isolated from wild snakes in
508 Taiwan reside within clade II (Sun et al. 2021, Ladner et al. 2022), which could also indicate a
509 southeast Asian origin for that clade, raising the possibility that clade II is not native to Europe.

510 Clade II has been detected on captive snakes in Europe (Ladner et al. 2022), which could serve
511 as a source for transmission into wild populations. An introduction of clade II into Europe
512 sometime before 1960 and subsequent spread could explain the wide distribution of this clade as
513 detected in our sampling. We detected two genotypes within clade II. One of these (II-D/E) was
514 widely distributed, whereas the other (II-F) was detected in a single snake community around a
515 lake in Switzerland. That snake community includes an introduced population of *N. tessellata*.
516 Taken together, this could indicate that genotype II-F was more recently introduced to Europe,
517 perhaps through the release of snakes originating in captivity. However, determining the genetic
518 diversity and origin of the various lineages of *O. ophidiicola* in Europe would require more in-
519 depth studies.
520 We find several disease hotspots in Europe, which could be attributed, at least partially,
521 to specific host species and the presence of distinct pathogen clades. The shape of this
522 relationship varied among areas with higher disease prevalence, and in some cases, host species
523 had higher infections regardless of pathogen genotypes, and others were likely attributed to the
524 presence of specific susceptible hosts infected with a pathogen clade that may be more
525 transmissible. Although virulence is recognized as an important factor in the effects of disease on
526 host populations, the general lack of landscape level data on pathogen lineage distribution and
527 association with disease has likely limited our ability to determine its importance for other
528 disease hotspots.
529
530 **Ethics**
531 Handling of snakes was reviewed and approved by Virginia Tech Institute for Animal Care and
532 Use Committee protocol 20-055. Permits to conduct our field study were obtained when

necessary, and were granted by the Regional office of the Karlovarian region, Department of Environment and Agriculture in Czech Republic (permit # KK/1098/ZZ/20-4), the General and Regional Directorates of Nature Conservation in Poland (permit # DZP- WG.6401.91.2020.TŁ; DZP-WG.6401.91.2020.TŁ.2, WPN.6401.270.2019.MF, WPN.6401.17.2020.KW.2, WPN.6401.9.2021.KW.2), Portuguese and Spanish wildlife legislation (permits # 295/2020/CAPT, 146/2021/CAPT, 201999902471003/IRM/MDCG/mes, EB-018/2020, EB-015/2021, AUES/CYL/192/2020, AUES/CYL/54/2021, A/2021/036, 0001-0261-2021-000003), the Direction régionale de l'environnement of Franche-Comte (ONAGRE 2020-01-17-00122; 25-2022-02-17-00001) and Loire-Atlantique (Cerfa 13616, permit # 64/2016) in France, the Museum of Natural History in Budapest, Hungary (permit # PE-KTFO/1568-18/2020), Austrian legislations (permits # MA22 – 1089768-2020, RU5-BE-64/023-2022, RU5-BE-64//022-2021, ABT13-53W-50/2018-2), the Federal Office for the Environment (FOEN) in Switzerland with veterinary authorization (VD3718, ID 33612), and cantonal authorizations (Neuchatel: FS-08/2021, Grisons: AV-2022-338, Vaud: 2021-3537).

Funding

This material is based upon work supported by the National Science Foundation Graduate Research Fellowship under Grant No. 480040. Additional funding to GB was provided by a Virginia Tech Cunningham fellowship, and a CeZAP (Center for Emerging, Zoonotic, and Arthropod-borne Pathogens) grant as part of the Infectious Diseases (ID) Interdisciplinary Graduate Education Program (IGEP). FM-F is supported by FCT - Fundação para a Ciência e a Tecnologia, Portugal (contract ref. DL57/2016/CP1440/CT0010). Sampling in Poland was funded by the statutory funds of the Institute of Nature Conservation, Polish Academy of

Science. Sampling in Hungary was supported by Duna-Ipoly National Park, Duna-Dráva National Park, Aggtelek National Park, and LIFE HUNVIPHAB project (LIFE18NAT/HU/000799). Sampling in France was funded by the Agence de l'eau Rhône-Méditerranée-Corse, Région Bourgogne-Franche-Comté, DREAL Bourgogne-Franche-Comté, Département du Jura, Doubs and Territoire de Belfort, and UNICEM (to AM and TC), and by the Regional Council of Nouvelle-Aquitaine and Aquastress project (2018-1R20214 to OL).

Acknowledgements

We thank Otto Aßmann, Florian Bacher, Jacek Błachuta, Philomin Briot, Jon Buldain, Maxime Chèvre, Pierre Cheveau, Sylvain Dubey, Anna Egerer, Lea Endrejat, Karin Ernst, Niklas Franzen, Inês Freitas, Georg Gassner, Davy Guinchard, Krisztián Harmos, Marietta Hengl, Piotr Hubal, Kacper Jurczyk, Yurii Kornilev, Roman Kurek, Nahla Lucchini, Adrian Neumann, Daniel Renner, Sandra Wallner, and Bartłomiej Zając for assistance in the field. Many thanks also to Kate Langwig for statistical insights, and to Oleksandra Klynova and Megan Winzeler for laboratory assistance.

Author contributions

GB: conceptualization, data curation, investigation, formal analysis, visualization, methodology, writing—original draft, writing—review and editing; JML: methodology, investigation, writing—review and editing; NJ: methodology, resources, investigation, writing—review and editing; SB: investigation, resources, writing—review and editing; TC: methodology, investigation, writing—review and editing; MF: investigation, writing—review and editing; FM-F: investigation, writing—review and editing; GG: investigation, writing—review and editing;

579 BH: investigation, writing—review and editing; AK: investigation, writing—review and editing;
580 KK: investigation, writing—review and editing; OL: investigation, writing—review and editing;
581 AM: methodology, investigation, writing—review and editing; RM: investigation, writing—
582 review and editing; SS: investigation, review and editing; BS: investigation, writing—review and
583 editing; SU: methodology, resources, investigation, writing—review and editing; OZ:
584 investigation, writing—review and editing; JRH: conceptualization, resources, supervision,
585 funding acquisition, writing—review and editing.
586

587 **Disclaimer**

588 Any use of trade, firm, or product names is for descriptive purposes only and does not imply
589 endorsement by the U.S. Government.
590

591 **Data availability statement**: The datasets and code generated for this study will be made
592 available in Dryad Digital Repository upon final submission.
593

594 **Conflict of interest declaration**

595 The authors declare no competing interests.
596

597 **References:**

598 Allender, M. C., M. Dreslik, S. Wylie, C. Phillips, D. B. Wylie, C. Maddox, M. A. Delaney, and
599 M. J. Kinsel. 2011. *Chrysosporium* sp. infection in eastern massasauga rattlesnakes.
600 Emerging Infectious Diseases **17**:2383.

601 Allender, M. C., D. B. Raudabaugh, F. H. Gleason, and A. N. Miller. 2015. The natural history,
602 ecology, and epidemiology of *Ophidiomyces ophiodiicola* and its potential impact on
603 free-ranging snake populations. Fungal Ecology **17**:187-196.
604 Allender, M. C., M. J. Ravesi, E. Haynes, E. Ospina, C. Petersen, C. A. Phillips, and R. Lovich.
605 2020. Ophidiomycosis, an emerging fungal disease of snakes: Targeted surveillance on
606 military lands and detection in the western US and Puerto Rico. PLoS One **15**:e0240415.
607 Ashford, R. W. 2003. When is a reservoir not a reservoir? Emerg Infect Dis **9**:1495-1496.
608 Baker, S. J., E. Haynes, M. Gramhofer, K. Stanford, S. Bailey, M. Christman, K. Conley, S.
609 Frasca, R. J. Ossiboff, and D. Lobato. 2019. Case definition and diagnostic testing for
610 snake fungal disease. Herpetological Review **50**:279-285.
611 Balaz, V., J. Vörös, P. Civis, J. Vojar, A. Hettyey, E. Sos, R. Dankovics, R. Jehle, D. G.
612 Christiansen, F. Clare, M. C. Fisher, T. W. Garner, and J. Bielby. 2014. Assessing risk
613 and guidance on monitoring of *Batrachochytrium dendrobatidis* in Europe through
614 identification of taxonomic selectivity of infection. Conserv Biol **28**:213-223.
615 Becker, C. G., S. E. Greenspan, K. E. Tracy, J. A. Dash, C. Lambertini, T. S. Jenkinson, D. S.
616 Leite, L. F. Toledo, J. E. Longcore, T. Y. James, and K. R. Zamudio. 2017. Variation in
617 phenotype and virulence among enzootic and panzootic amphibian chytrid lineages.
618 Fungal Ecology **26**:45-50.
619 Bohuski, E., J. M. Lorch, K. M. Griffin, and D. S. Blehert. 2015. TaqMan real-time polymerase
620 chain reaction for detection of *Ophidiomyces ophiodiicola*, the fungus associated with
621 snake fungal disease. BMC Veterinary Research **11**:95.
622 Brown, V. L., J. M. Drake, D. E. Stallknecht, J. D. Brown, K. Pedersen, and P. Rohani. 2013.
623 Dissecting a wildlife disease hotspot: the impact of multiple host species, environmental

transmission and seasonality in migration, breeding and mortality. J R Soc Interface **10**:20120804.

Burbrink, F. T., J. M. Lorch, and K. R. Lips. 2017. Host susceptibility to snake fungal disease is highly dispersed across phylogenetic and functional trait space. Science Advances **3**:e1701387.

Bürkner, P. C. 2017. brms: An R package for Bayesian multilevel models using Stan. Journal of Statistical Software **80**:1-28.

Chandler, H. C., M. C. Allender, B. S. Stegenga, E. Haynes, E. Ospina, and D. J. Stevenson. 2019. Ophidiomycosis prevalence in Georgia's Eastern Indigo Snake (*Drymarchon couperi*) populations. PLoS One **14**:e0218351.

Davy, C. M., L. Shirose, D. Campbell, R. Dillon, C. McKenzie, N. Nemeth, T. Braithwaite, H. Cai, T. Degazio, T. Dobbie, S. Egan, H. Fotherby, J. D. Litzgus, P. Manorome, S. Marks, J. E. Paterson, L. Sigler, D. Slavic, E. Slavik, J. Urquhart, and C. Jardine. 2021. Revisiting Ophidiomycosis (snake fungal disease) after a decade of targeted research. Front Vet Sci **8**:665805.

Dorcas, M. E., and J. D. Willson. 2009. Innovative methods for studies of snake ecology and conservation. Snakes: Ecology and Conservation:5-37.

Dubey, S., S. Pellaud, K. Gindro, J. Schuerch, J. Golay, R. Gloor, K. Ghali, and O. Dubey. 2022. Fungal infection in free-ranging snakes caused by opportunistic species. Emerging Animal Species **3**:100001.

Franklinos, L. H., J. M. Lorch, E. Bohuski, J. R.-R. Fernandez, O. N. Wright, L. Fitzpatrick, S. Petrovan, C. Durrant, C. Linton, and V. Baláž. 2017. Emerging fungal pathogen *Ophidiomyces ophiodiicola* in wild European snakes. Scientific Reports **7**:1-7.

647 Gandon, S., and Y. Michalakis. 2000. Evolution of parasite virulence against qualitative or
648 quantitative host resistance. Proc Biol Sci **267**:985-990.
649 Greener, M. S., E. Verbrugghe, M. Kelly, M. Blooi, W. Beukema, S. Canessa, S. Carranza, S.
650 Croubels, N. De Troyer, D. Fernandez-Giberteau, P. Goethals, L. Lens, Z. Li, G. Stegen,
651 D. Strubbe, R. van Leeuwenberg, S. Van Praet, M. Vila-Escale, M. Vervaeke, F.
652 Pasmans, and A. Martel. 2020. Presence of low virulence chytrid fungi could protect
653 European amphibians from more deadly strains. Nat Commun **11**:5393.
654 Grioni, A., K. W. To, P. Crow, L. Rose-Jeffreys, L. O. Chu, F. I. Hill, H. K. Chan, and K. S.
655 Cheung. 2021. Detection of *Ophidiomyces ophidiicola* in a wild Burmese python (*Python*
656 *bivittatus*) in Hong Kong SAR, China. The Journal of Herpetological Medicine and
657 Surgery **31**:283-291.
658 Hawley, D. M., E. E. Osnas, A. P. Dobson, W. M. Hochachka, D. H. Ley, and A. A. Dhondt.
659 2013. Parallel patterns of increased virulence in a recently emerged wildlife pathogen.
660 PLoS Biol **11**:e1001570.
661 Haydon, D. T., S. Cleaveland, L. H. Taylor, and M. K. Laurenson. 2002. Identifying reservoirs
662 of infection: A conceptual and practical challenge. Emerging Infectious Diseases **8**:1468-
663 1473.
664 Haynes, E., H. C. Chandler, B. S. Stegenga, L. Adamovicz, E. Ospina, D. Zerpa-Catanho, D. J.
665 Stevenson, and M. C. Allender. 2020. Ophidiomycosis surveillance of snakes in Georgia,
666 USA reveals new host species and taxonomic associations with disease. Scientific
667 Reports **10**:1-15.

668 Holdo, R. M., A. R. E. Sinclair, A. P. Dobson, K. L. Metzger, B. M. Bolker, M. E. Ritchie, and
669 R. D. Holt. 2009. A disease-mediated trophic cascade in the serengeti and its implications
670 for ecosystem C. Plos Biology **7**.
671 Hyatt, A. D., D. G. Boyle, V. Olsen, D. B. Boyle, L. Berger, D. Obendorf, A. Dalton, K. Kriger,
672 M. Hero, H. Hines, R. Phillott, R. Campbell, G. Marantelli, F. Gleason, and A. Colling.
673 2007. Diagnostic assays and sampling protocols for the detection of *Batrachochytrium*
674 *dendrobatidis*. Diseases of Aquatic Organisms **73**:175-192.
675 Kilpatrick, A. M., A. A. Chmura, D. W. Gibbons, R. C. Fleischer, P. P. Marra, and P. Daszak.
676 2006. Predicting the global spread of H5N1 avian influenza. Proceedings of the National
677 Academy of Sciences of the United States of America **103**:19368-19373.
678 Krauss, S., D. E. Stallknecht, N. J. Negovetich, L. J. Niles, R. J. Webby, and R. G. Webster.
679 2010. Coincident ruddy turnstone migration and horseshoe crab spawning creates an
680 ecological 'hot spot' for influenza viruses. Proc Biol Sci **277**:3373-3379.
681 LaDeau, S. L., A. M. Kilpatrick, and P. P. Marra. 2007. West Nile virus emergence and large-
682 scale declines of North American bird populations. Nature **447**:710-713.
683 Ladner, J. T., J. M. Palmer, C. L. Ettinger, J. E. Stajich, T. M. Farrell, B. M. Glorioso, B.
684 Lawson, S. J. Price, A. G. Stengle, D. A. Grear, and J. M. Lorch. 2022. The population
685 genetics of the causative agent of snake fungal disease indicate recent introductions to the
686 USA. PLoS Biol **20**:e3001676.
687 Laggan, N. A., K. L. Parise, J. P. White, H. M. Kaarakka, J. A. Redell, J. E. DePue, W. H.
688 Scullon, J. Kath, J. T. Foster, A. M. Kilpatrick, K. E. Langwig, and J. R. Hoyt. 2022.
689 Host abundance and heterogeneity in infectiousness determine extent of the
690 environmental reservoir. bioRxiv:2022.2009.2020.508714.

691 Langwig, K. E., W. F. Frick, J. T. Bried, A. C. Hicks, T. H. Kunz, and A. M. Kilpatrick. 2012.
692 Sociality, density-dependence and microclimates determine the persistence of
693 populations suffering from a novel fungal disease, white-nose syndrome. Ecol Lett **15**.
694 Langwig, K. E., J. R. Hoyt, K. L. Parise, W. F. Frick, J. T. Foster, and A. M. Kilpatrick. 2017.
695 Resistance in persisting bat populations after white-nose syndrome invasion.
696 Philosophical Transactions of the Royal Society B: Biological Sciences **372**:20160044.
697 Li, K. S., Y. Guan, J. Wang, G. J. Smith, K. M. Xu, L. Duan, A. P. Rahardjo, P. Puthavathana, C.
698 Buranathai, T. D. Nguyen, A. T. Estoepangestie, A. Chaisingh, P. Auewarakul, H. T.
699 Long, N. T. Hanh, R. J. Webby, L. L. Poon, H. Chen, K. F. Shortridge, K. Y. Yuen, R. G.
700 Webster, and J. S. Peiris. 2004. Genesis of a highly pathogenic and potentially pandemic
701 H5N1 influenza virus in eastern Asia. Nature **430**:209-213.
702 Lorch, J. M., S. Knowles, J. S. Lankton, K. Michell, J. L. Edwards, J. M. Kapfer, R. A. Staffen,
703 E. R. Wild, K. Z. Schmidt, and A. E. Ballmann. 2016. Snake fungal disease: an emerging
704 threat to wild snakes. Philosophical Transactions of the Royal Society B: Biological
705 Sciences **371**:20150457.
706 Marini, D., M. R. Di Nicola, V. Crocchianti, T. Notomista, D. Iversen, L. Coppari, M. Di
707 Criscio, V. Brouard, J.-L. C. M. Dorne, J. Rüegg, and M. L. Marenzoni. 2023. Pilot
708 survey reveals ophidiomycosis in dice snakes Natrix tessellata from Lake Garda, Italy.
709 Veterinary Research Communications. https://doi.org/10.1007/s11259-023-10129-7
710 McClure, K. M., R. C. Fleischer, and A. M. Kilpatrick. 2020. The role of native and introduced
711 birds in transmission of avian malaria in Hawaii. Ecology **101**:e03038.

712 McKenzie, J. M., S. J. Price, J. L. Fleckenstein, A. N. Drayer, G. M. Connette, E. Bohuski, and J.
713 M. Lorch. 2019. Field diagnostics and seasonality of *Ophidiomyces ophiodiicola* in wild
714 snake populations. Ecohealth **16**:141-150.
715 McLeod, D. V., and S. Gandon. 2022. Effects of epistasis and recombination between vaccine-
716 escape and virulence alleles on the dynamics of pathogen adaptation. Nat Ecol Evol
717 **6**:786-793.
718 Meier, G., T. Notomista, D. Marini, and V. Ferri. 2018. First case of Snake Fungal Disease
719 affecting a free-ranging *Natrix natrix* (LINNAEUS, 1758) in Ticino Canton, Switzerland.
720 Herpetology Notes **11**:885-891.
721 O'Hanlon, S. J., A. Rieux, R. A. Farrer, G. M. Rosa, B. Waldman, A. Bataille, T. A. Kosch, K.
722 A. Murray, B. Brankovics, and M. Fumagalli. 2018. Recent Asian origin of chytrid fungi
723 causing global amphibian declines. Science **360**:621-627.
724 Origgi, F. C., S. R. R. Pisano, O. Glaizot, S. T. Hertwig, A. Schmitz, and S. Ursenbacher. 2022.
725 *Ophidiomyces ophiodiicola*, the etiologic agent of snake fungal disease, is present in
726 Europe since the late 1950's. Emerging Infectious Diseases **28**.
727 Pandey, A., N. Mideo, and T. G. Platt. 2022. Virulence evolution of pathogens that can grow in
728 reservoir environments. Am Nat **199**:141-158.
729 Paull, S. H., S. Song, K. M. McClure, L. C. Sackett, A. M. Kilpatrick, and P. T. J. Johnson.
730 2012. From superspreaders to disease hotspots: linking transmission across hosts and
731 space. Frontiers in Ecology and the Environment **10**:75-82.
732 R Core Team. 2022. R: A language and environment for statistical computing. R Foundation for
733 Statistical Computing, Vienna, Austria. URL https://www.R-project.org/.

734 Ribeiro, L. P., T. Carvalho, C. G. Becker, T. S. Jenkinson, D. D. S. Leite, T. Y. James, S. E.
735 Greenspan, and L. F. Toledo. 2019. Bullfrog farms release virulent zoospores of the frog-
736 killing fungus into the natural environment. Scientific Reports **9**:13422.
737 Schneider, C. A., W. S. Rasband, and K. W. Eliceiri. 2012. NIH Image to ImageJ: 25 years of
738 image analysis. Nat Methods **9**:671-675.
739 Sun, P. L., C. K. Yang, W. T. Li, W. Y. Lai, Y. C. Fan, H. C. Huang, and P. H. Yu. 2021.
740 Infection with *Nannizziopsis guarroi* and *Ophidiomyces ophiodiicola* in reptiles in
741 Taiwan. Transboundary and Emerging Diseases **69**:764-775.
742 Sutherland, W. J., R. Aveling, T. M. Brooks, M. Clout, L. V. Dicks, L. Fellman, E. Fleishman,
743 D. W. Gibbons, B. Keim, and F. Lickorish. 2014. A horizon scan of global conservation
744 issues for 2014. Trends in ecology & evolution **29**:15-22.
745 Urbina, J., E. M. Bredeweg, T. S. Garcia, and A. R. Blaustein. 2018. Host–pathogen dynamics
746 among the invasive American bullfrog (*Lithobates catesbeianus*) and chytrid fungus
747 (*Batrachochytrium dendrobatidis*). Hydrobiologia **817**:267-277.
748 van Riper, C., S. G. van Riper, M. L. Goff, and M. Laird. 1986. The epizootiology and
749 ecological significance of malaria in Hawaiian land birds. Ecological Monographs
750 **56**:327-344.
751 Voyles, J., S. Young, L. Berger, C. Campbell, W. Voyles, A. Dinudom, D. Cook, R. Webb, R.
752 Alford, L. Skerratt, and R. Speare. 2009. Pathogenesis of chytridiomycosis, a cause of
753 catastrophic amphibian declines. Science **326**:582 - 585.
754 White, T. J., T. Bruns, S. Lee, and J. Taylor. 1990. Amplification and direct sequencing of fungal
755 ribosomal RNA genes for phylogenetics. Pages 315-322 *in* M. A. Innis, D. H. Gelfland, J.

756 J. Sninsky, and T. J. White, editors. PCR Protocols: A Guide to Methods and
757 Applications. Academic Press Inc., San Diego, CA.
758 Wilber, M. Q., P. T. J. Johnson, and C. J. Briggs. 2020. Disease hotspots or hot species?
759 Infection dynamics in multi-host metacommunities controlled by species identity, not
760 source location. Ecol Lett **23**:1201-1211.
761